

## MAGNETIC BARKHAUSEN EMISSION ANALYSIS FOR ASSESSMENT OF MICROSTRUCTURES AND DAMAGE

Baldev Raj, T.Jayakumar and S.Vaidyanathan

Metallurgy and Materials Group, Indira Gandhi Centre for Atomic Research, Kalpakkam, India

**Abstract:** Application of magnetic Barkhausen emission (MBE) analysis for assessment of microstructures and damage in various materials including carbon steel, Cr-Mo ferritic steels, 17-4 PH steel and metastable austenitic stainless steel has been highlighted in this paper. Thermally induced microstructural changes in Cr-Mo steels have been correlated with MBE, based on a two stage magnetization process model. The MBE parameters have also been used to characterise different stages of tensile deformation and to assess tensile strength, Charpy impact energy, quality of induction hardening process, progress of carburization in reformer tubes and fatigue damage.

**Introduction:** The characterization of microstructures, mechanical properties, deformation, damage initiation and growth by Non-Destructive Evaluation (NDE) techniques is assuming a vital role in various industries because of the growing awareness of the benefits that can be derived by using NDE techniques for assessing the performance of various components. Fracture mechanics based analysis of component integrity requires quantitatively characterization of microstructure, defects as well as stresses. Any alteration in the microstructure, which reduces the life or performance, should be predicted sufficiently in advance in order to ensure safe, reliable and economic operation of the components. This prediction is possible with NDE techniques, when it is realised that the interaction of the nondestructive probing medium with the material depends on the substructural / microstructural features such as point defects, dislocations, voids, micro and macro cracks, secondary phases, texture and residual stress. In this paper, use of MBE technique for characterization of microstructures, deformation and fatigue damage in different steels is discussed.

**Assessment of Grain/ Lath Size and Carbide Size Associated with Thermal Ageing in Ferritic Steels:** During thermal aging of ferritic steel components operating at higher temperatures, the dislocation density, size and distribution of laths / grains and second phase precipitates would vary in a synergistic manner. Using MBE parameters, a two-stage magnetization process has been proposed in sufficiently tempered microstructures, considering the grain boundaries and the carbide precipitates as the two major types of obstacles to the domain wall movement. The model has been used to characterise the tempered microstructures on the MBE behaviour in carbon steel, 2.25Cr-1Mo steel and 9Cr-1Mo steels [1].

The variation in the RMS voltage of the MBE with current applied to the electromagnetic yoke systematically changes from a single peak to two peaks with increase in tempering time in carbon steel and Cr-Mo steels. Figures 1(a, b) typically show the results obtained for 0.3% carbon steel [1]. Based on the two-stage magnetization process model proposed, the MBE peak 1 has been attributed to influence of grain boundaries and the peak 2 to that of carbides [1, 2]. As per this model, the grain boundaries and precipitates would act as obstacles to the domain wall movement in different field ranges and two peaks in the MBE profile have been observed for these steels in sufficiently tempered condition. The systematic changes in the height and position of these two MBE peaks at different stages of tempering have been explained based on the variations in the lath/grain size and type and size of carbides [1, 2]. Since the formation and growth of reverse domains would become more and more easy with the increase in grain size due to large demagnetizing field at the grain boundaries and hence, the MBE peak 1 position would shift to lower magnetic field as, shown in Fig. 1(a, b). Similarly, with increasing tempering time, the carbide size increases. The carbides with higher size offer more resistance to domain wall movement and hence the field corresponding to peak 2 shifts to higher field, as shown in Fig. 1(a, b). Excellent correlations between positions of MBE peaks 1 and 2 and microstructural parameters (grain/lath size and carbide size) have been obtained, as shown in Figs. 2(a, b). These results indicate that the MBE technique can be used to evaluate the changes in the grain size and precipitate size in long-term aged ferritic steels. However, this is difficult in short-term aged conditions, where the dislocation density is high, and the lath and precipitate sizes are very small.

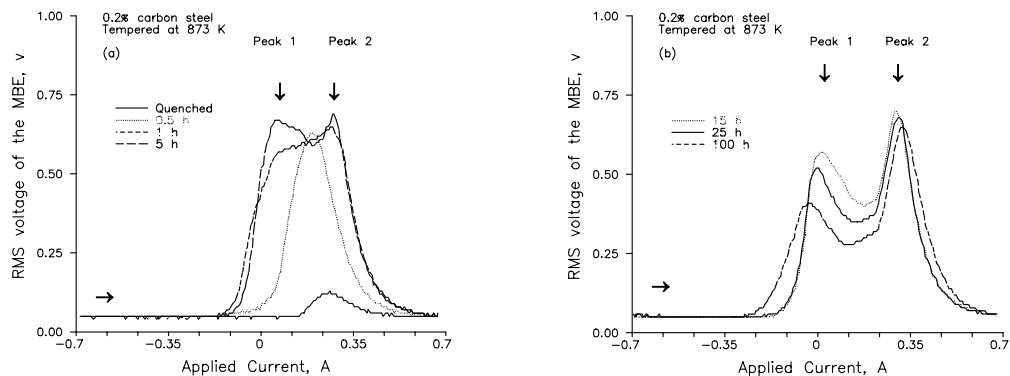


Fig. 1(a-b). Variation in the RMS voltage of the MBE for different tempered 0.2% carbon steel samples.

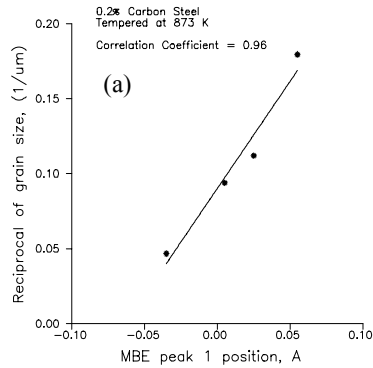


Fig. 2(a). Relationship between the MBE peak 1 position and average grain size for different tempered 0.2% carbon steel samples.

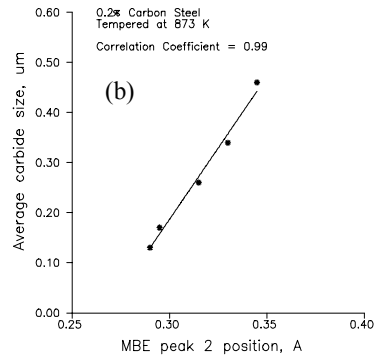


Fig. 2(b). Relationship between the MBE peak 2 position and the average size of cementite precipitates for different tempered 0.2% carbon steel samples.

**Influence of Morphology of Cementite in 0.3% Carbon Steel:** Studies have been carried out in annealed and thermally aged 0.3 % carbon steel samples to establish the effect of lamellar and spheroidized cementite structures on MBE behaviour [3]. The annealed sample having ferrite and pearlite microstructure showed a sharp slope change near the field transition and a dominant peak in the MBE profile whereas the thermally aged sample having spheroidized cementite particles showed two peaks in the MBE profile (Fig. 3).

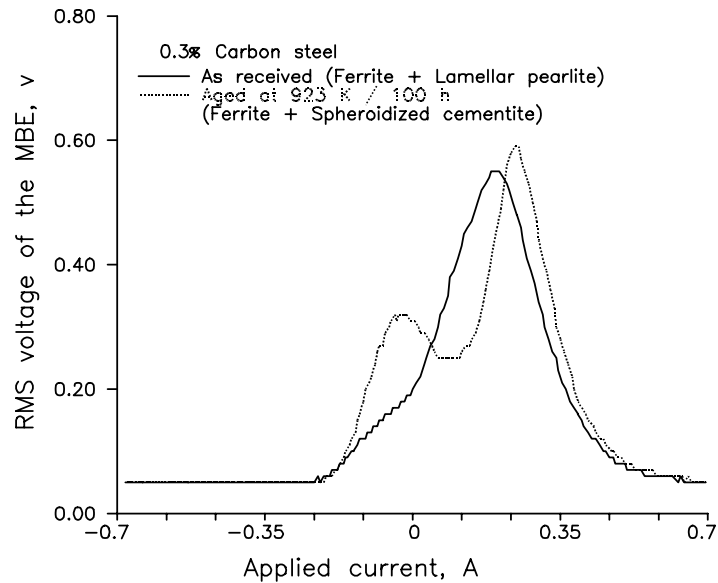


Fig. 3. Difference in the RMS voltage profile of the MBE for lamellar and spheroidized cementite structures in 0.3% carbon steel.

The microstructural observations clearly showed that, every ferrite grain is covered with lamellar cementite boundaries on at least two sides. Hence, even in the ferrite grains, the domain walls can not move to larger distance as they are restricted by the pinning of domain walls by the grain boundaries with lamellar cementite. Therefore, the small peak (slope change) near the field transition in the MBE profile can be attributed to the domain wall movement in overcoming the resistance offered by ferrite grain boundary (without precipitates) before they are pinned by the grain boundaries with lamellar precipitates. The dominant peak at higher field is attributed to the domain walls overcoming the resistance offered by the grain boundaries with lamellar precipitates. The spheroidization of cementite during thermal aging increases the precipitate-free ferrite grain boundaries and hence the first MBE peak height near the field transition. The second peak becomes narrow and shifts to higher field indicating the spheroidization of cementites and their stronger resistance to domain wall movement.

**Identification of Various Stages of Tensile Deformation in Ferritic Steels:**

Studies have been carried out to characterise the tensile deformation in ferritic steels using the MBE analysis [4]. These studies indicated four different stages of tensile deformation, namely, (i) perfectly elastic, (ii) micro-plastic yielding, (iii) macro yielding, and (iv) progressive plastic deformation. Figure 4 shows the effect of different stages of prior tensile deformation on the MBE profile in

tempered 2.25Cr-1Mo steel. It can be observed that the MBE profile remains more or less same up to certain stress level. Then, with the increase in prior applied stress level, both MBE peak 1 and peak 2 height values decrease. On further increase in prior stress level, the initially present two peaks in the MBE profile merge into a single peak in between the originally present two peaks. Beyond macro yielding, the single central MBE peak decreases gradually with prior tensile stress level. Fig. 5 shows the variation in the MBE peak height and the prior stress level as a function of strain in tempered 2.25Cr-1Mo steel. The different stages of progressive tensile deformation are clearly brought out from this illustration

**Stage 1 – Perfectly elastic region:** It can be observed from Fig. 4 that, during initial stages of elastic loading, the MBE profiles remain comparable to that of the virgin condition. This indicates the fact that there is no significant change in the microstructure (dislocation density) after unloading from these stress levels. The constant values of MBE peak 1 height in the unloaded condition (stage 1 in Figs. 4 and 5) confirm that the stage 1 to be in perfectly elastic condition.

**Stage 2 – Micro-yielding:** It can be seen from Fig. 4 that the height of both the MBE peak 1 and peak 2 decrease significantly well before the macro yielding. This indicates the activation of grain boundary and Frank-Read type dislocation sources even during the macro-elastic region (about 3/4 of the yield stress) causing the micro-plastic yielding. The dislocation pile-ups created within the grain would reduce the mean free path of domain wall displacement and hence the MBE peak heights.

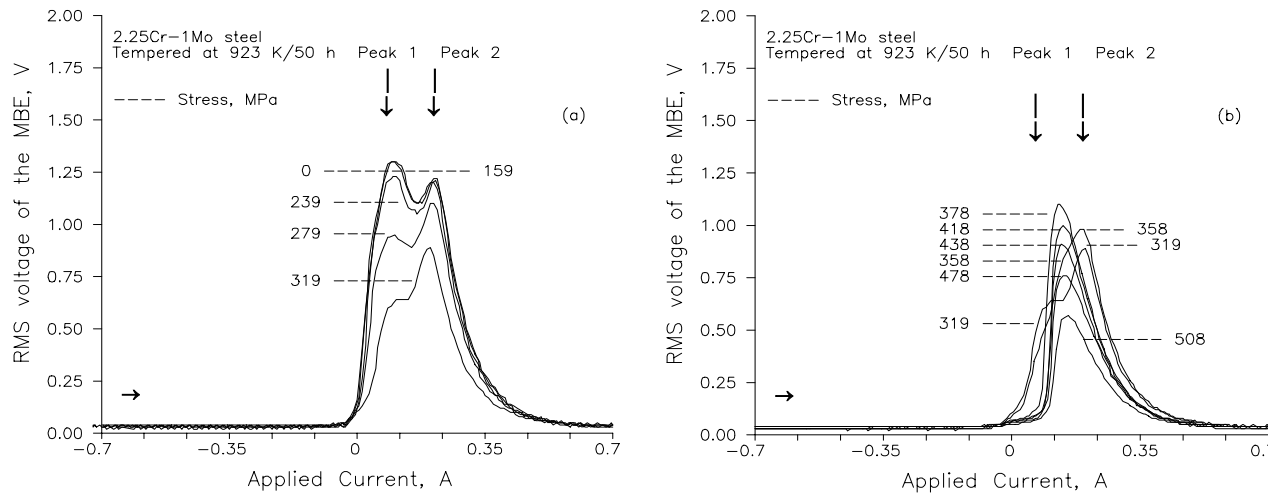


Fig. 4(a-b). Variations in the RMS voltage profile of the MBE for different prior stress levels of tensile deformation in a tempered 2.25Cr-1Mo steel.

**Stage 3 – Macro-yielding:** Near the macro yielding, the originally present two MBE peaks merge into single central peak with relatively higher peak height and narrow profile width. It is known that the macro yielding is associated with grain rotation in order to maintain the boundary integrity between the adjacent grains for compatible deformation. When such grain rotation occurs under the action of external tensile stress, the grain reorientation would be such that the  $\langle 100 \rangle$  direction in some grains would tend to align closer to the stress

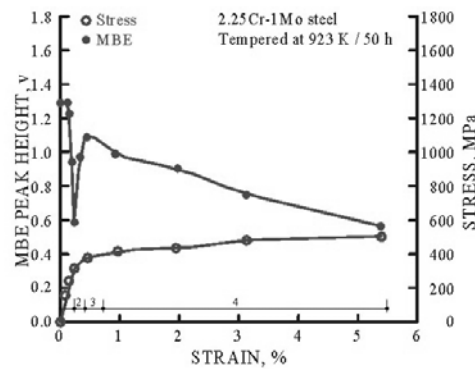


Fig. 5. Typical variation in the MBE level, magnetic flux density and the applied stress as a function of percentage nominal strain in quenched and tempered 2.25 Cr-1Mo steel specimen

direction in order to reduce its magneto static energy by way of decreasing the normal component of magnetization across the grain boundary.

This results in domain alignment closer to the tensile stress direction and would enhance domain wall movement during magnetization along the stress direction and hence the increase in the micro-magnetic parameters.

**Stage 4 – Progressive plastic deformation:** The entry into the plastic deformation regime is clearly reflected by gradual decrease in the MBE peak height. The dislocations generated due to plastic deformation act as strong obstacles to domain wall movement. The plastic deformation is associated with formation of extensive dislocation tangles, which would reduce the mean free path of the domain wall displacement. The linear reduction in the MBE peak with strain is attributed to the increase in the dislocation density and the compressive residual stress produced on the surface due to the prior tensile deformation.

**Assessment of Induction Hardened Specimens:** Studies have also been carried out on understanding the MBE behaviour in induction hardened

specimens with a view to develop a MBE based method for qualifying induction hardened components [5]. These studies have demonstrated that it is possible to detect the co-existence of hard and soft ferromagnetic phases (for example, martensite and ferrite) from the observed two-peak MBE profile (Fig. 6(a)). The variation in the volume fraction of ferrite and martensite phases with in the hardened region could be directly correlated to the height variation of the two peaks in the MBE profile (Fig. 6(b)). This method not only gives the case depth but also the quality of the case depth with respect to the microstructure consisting of ferrite and martensite phases.

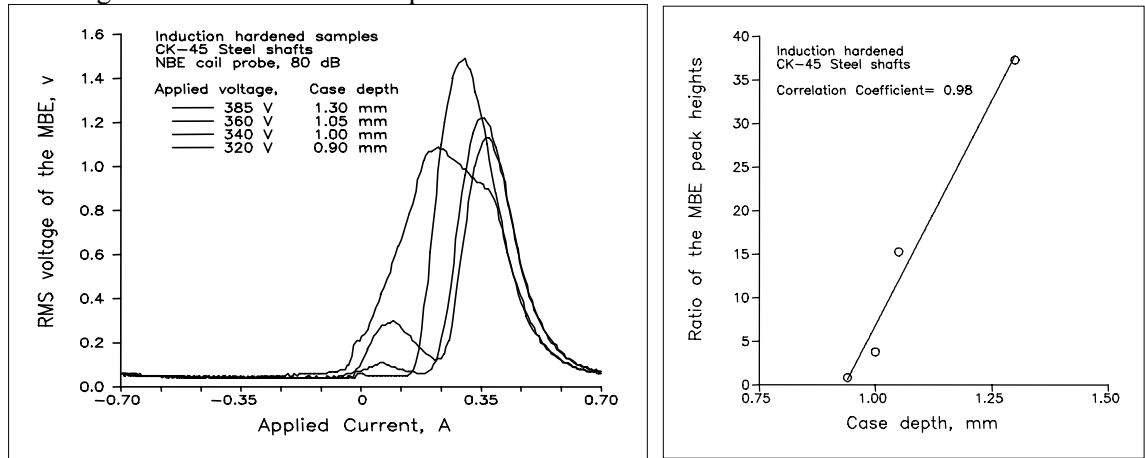


Fig. 6. (a) Variation in the rms voltage of the MBE signal with applied current at different voltages used for induction hardening and (b) Variation in the ratio of the MBE peak heights with case depth of the induction hardened shafts made of CK-45 steel.

**Assessment of Progress of Carburisation in Reformer Tubes:** MBE measurements have been made for the evaluation of carburization depth in 0.5Cr-0.5Mo ferritic steel reformer tubes (130 mm outside diameter and 8 mm wall thick) used in petrochemical industry [6]. The measurements have been carried out on sample pieces (100 mm long and 10 mm wide) taken out from tubes exposed in service, at different depths (cross section) from carburised inside surface of the tube to simulate the variation in carbon concentration gradient within the skin depth of MBE with increasing time of exposure to carburization. Fig. 7 shows the typical plot of rms voltage of MBE signal as a function of applied magnetic field at different locations along the thickness direction (cross section) of one pipe sample. The MBE level increases with increasing depth of measurement from the inside surface, i.e. maximum carburised region to non carburised region (Fig. 8). An inverse relationship between MBE voltage and hardness (hardness increases due to carbon pick up and carburization) has been observed This study suggests that the MBE

measurements on the carburised surface can be correlated with the concentration gradient within the skin depth of the MBE which (with proper prior calibration) would help in predicting the approximate depth of the carburised layer.

**Evaluation of Stress Induced Martensite in Metastable Austenitic Stainless Steels:** In the case of metastable austenitic steels, the stress induced ferromagnetic phase formation during cold working would contribute to the magnetization and hence to the MBE. The RMS voltage of the MBE signals for different cold

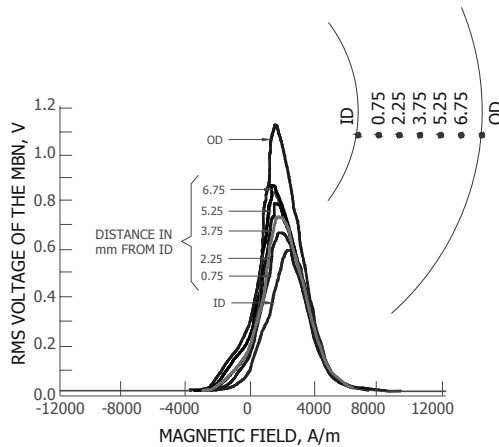


Fig. 7. Variation in MBE profile in specimens taken from different depths from the inside surface

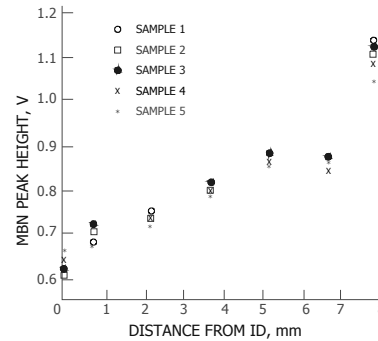


Fig. 8. Variation in MBE peak height with distance from the inside surface of the inservice carburised reformer tube

worked specimens of AISI type 304 Stainless steel has been measured at 50mHz and 1Hz applied field frequencies [7, 8]. There is gradual increase in peak height and broadening of the MBE signal with increase in the cold work (Fig. 9). Two parameters, half of the difference in the magnetic field corresponding to the two peaks of the MBE signal ( $H_{cm}$ ) and the maximum amplitude ( $M_{max}$ ) of the RMS voltage of the MBE signal were estimated. The  $M_{max}$  value was found to increase with increase in the degree of cold work and the frequency of applied magnetic field. The increase in  $M_{max}$  was more pronounced in specimens with higher degree of cold work (>20%) and at higher frequencies of applied field (1Hz and 10Hz). The increase in  $M_{max}$  with increase in frequency of magnetic field was attributed to the higher rate of movement of domain walls with increase in the applied field frequency causing higher induction in the pick up sensor. The increase in the  $M_{max}$  with increase in the degree of cold work is attributed to the increase in the amount of  $\alpha'$ -martensite. The MBE measurements can also be used, particularly at higher applied field frequency to detect the presence of  $\alpha'$  -martensite even in 10% cold worked

specimens. It was also established that MBE analysis could be utilized advantageously over hysteresis loop measurements for assessment of stress-induced  $\alpha'$ -martensite in nonstandard/irregular shaped objects/components and at localized regions.

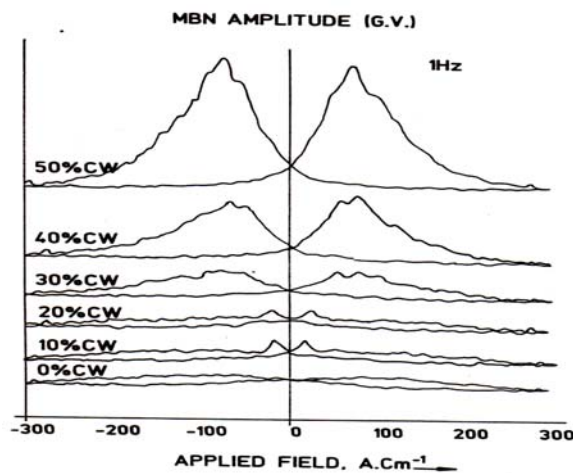


Fig. 9. Variation in RMS voltage of MBE signal with applied field for different cold worked AISI type 304 stainless steel.

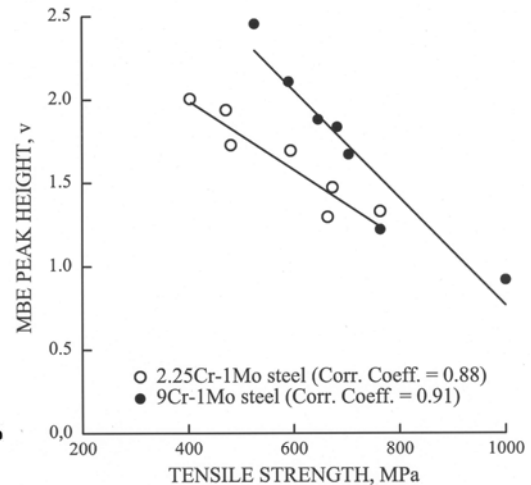


Fig. 10. Relationship between MBE peak height and Tensile strength in thermally aged and simulated HAZ microstructures of 2.25Cr-1Mo and 9Cr-1Mo steels

**Evaluation of Tensile Strength and Impact Toughness:** Studies have been carried out to relate the mechanical properties with MBE parameters in Cr-Mo ferritic steels and 17-4 PH steel [3]. The RMS voltage peak of the MBE profile has also been correlated to tensile strength in simulated heat affected zone microstructures of weldments of Cr-Mo steels (Fig. 10) and short-term thermally aged microstructures in 17-4PH steel (Fig. 11) and impact toughness in aged 17-4 PH steel (Fig. 12). In Cr-Mo steels, the MBE decreases with increase in tensile strength, but the reverse is observed for 17-4 PH steel. This is because, in Cr-Mo steel, dissolution of bainite or martensite is accompanied by coarsening of ferrite laths/grains. This would lead to reduction in tensile strength, but would enhance the domain wall displacement and hence the MBE. In the case of 17-4 PH steel, the thermal aging results in the austenite reversion in the copper-rich precipitate regions. The austenite formation would reduce the tensile strength, but strongly inhibits the domain alignment process and hence reduces the MBE. At the same time, the formation of austenite increases the impact toughness. These studies clearly show that the MBE behaviour is strongly influenced by the kind of microstructural evolution and its effect on

the magnetization process, rather than simply on hardening or softening process.

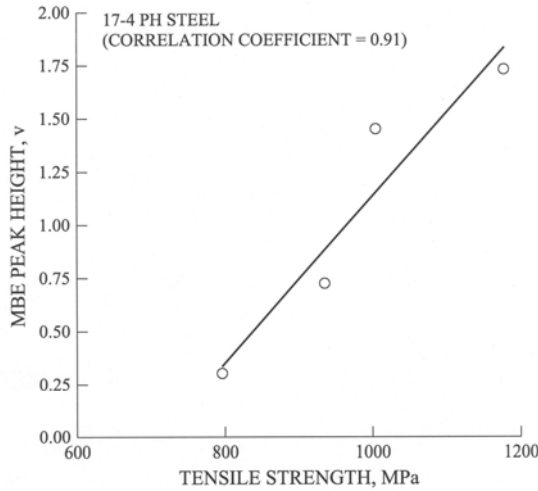


Fig. 11. Relationship between MBE peak height and Tensile strength in thermally aged 17-4PH steel

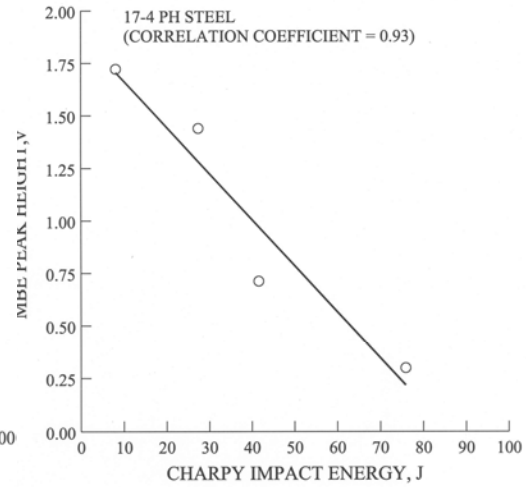


Fig. 12. Relationship between MBE peak height and Charpy impact energy in thermally aged 17-4PH steel.

**Assessment of Fatigue Damage:** Recently, the MBE technique has been used to assess the progressive low cycle fatigue (LCF) damage in 9Cr-1Mo ferritic steel [9]. Total strain controlled fatigue tests were conducted at ambient temperature employing plastic strain amplitudes of  $\pm 0.25$ ,  $\pm 0.50$  and  $\pm 0.75$  %. MBE measurements have been performed on LCF tested specimens interrupted at various life fractions. The various stages of deformation and fracture under LCF loading such as cyclic hardening, cyclic softening, saturation and surface crack initiation and propagation have been examined and identified using peak height value of the RMS voltage of the MBE. Figure 13 shows the variation in stress amplitude and MBE peak height at different stages of LCF life under three different strain amplitudes. The cyclic hardening, which occurred in the early stage of LCF cycling in 9Cr-1Mo steel, decreases the MBE peak height value. The reduction in MBE peak height value increased with increase in the amount of hardening, which in turn depends on strain amplitude. The progressive cyclic softening stage displayed reversal in MBE response i.e., the MBE peak height value increased with softening. Further, the saturation stage, where the stress value remained constant for a large number of cycles due to formation of stable dislocation substructure, results in a constant value of MBE. Finally, the onset of rapid stress drop and cusp formation in the stress-strain hysteresis loop, which indicates surface crack initiation and propagation,

exhibited a rapid increase in the MBE peak values. This is attributed to the movement of additional reverse domains produced at the crack surfaces. The rapid increase in MBE due to crack initiation and propagation has been confirmed by the measurement of MBE on the crack and away from the crack using surface MBE probe. These studies indicate that MBE can be used to monitor accumulation of fatigue damage on components exposed to cyclic loading and predict the remaining service life.

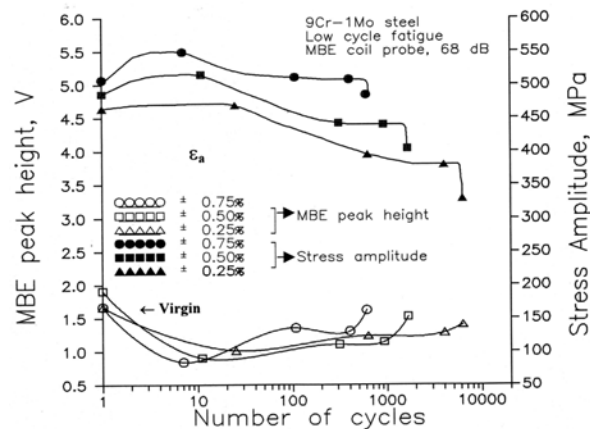


Fig. 13. Effect of low cycle fatigue on MBE

**Conclusion:** In this paper, the versatility of analysis of magnetic Barkhausen emission for characterization of microstructures and tensile deformation, evaluation of yield strength, impact toughness and fatigue damage, assessment of quality of induction hardening process and in-service damage due to carburization in reformer tubes has been highlighted.

#### References

- 1) V.Moorthy, S.Vaidyanathan, T. Jayakumar, Baldev Raj and B.P. Kashyap, *Metall. Mater. Trans. A*, 31, 2000, pp. 1053-1081.
- 2) V. Moorthy, S. Vaidyanathan, T. Jayakumar and Baldev Raj: *Philosophical Magazine A*, 77, 1998, pp. 1499-1514.
- 3) Baldev Raj, V.Moorthy, T.Jayakumar and K.Bhanu Sankara Rao, *International Materials Review*, 48, 2003, pp. 273-325.
- 4) V. Moorthy, S.Vaidyanathan, T. Jayakumar, Baldev Raj and B.P. Kashyap: *Acta Materialia*, 1999, 47 (6) 1999, pp. 1868-1879.
- 5) S.Vaidyanathan, V.Moorthy, T. Jayakumar and Baldev Raj: *Mater. Sci. Tech*, 2000, 16 (2) 202-208.
- 6) S.Vaidyanathan, V.Moorthy, T.Jayakumar and Baldev Raj, *Materials Evaluation*, 56, 1998, pp. 449-452.

- 7) T. Jayakumar, Ph.D. Thesis, Microstructural Characterization of Metallic Materials Using Ultrasonic and Magnetic methods, University of Saarland, Saarbrucken, Germany, 1996.
- 8) T. Jayakumar, T.D. Koble, W.A. Theiner and Baldev Raj: *Nondes. Test. Evaln.*, 1993, 10, 205-214.
- 9) V. Moorthy, B.K. Choudhary, S. Vaidyanathan, T. Jayakumar, K. Bhanusankara Rao and Baldev Raj, *Int. J. of Fatigue*, 21, 1999, pp. 263-269.